J|A|C|S
ARTICLES
Published on Web 04/24/2002

Conformationally Constrained Macrocycles That Mimic Tripeptide β-Strands in Water and Aprotic Solvents

Robert C. Reid, Michael J. Kelso, Martin J. Scanlon, and David P. Fairlie*

Contribution from the Centre for Drug Design and Development, Institute for Molecular Bioscience, University of Queensland, Brisbane, Qld 4072, Australia

Received January 19, 2002

Abstract: The β-strand conformation is unknown for short peptides in aqueous solution, yet it is a fundamental building block in proteins and the crucial recognition motif for proteolytic enzymes that enable formation and turnover of all proteins. To create a generalized scaffold as a peptidomimetic that is pre-organized in a β-strand, we individually synthesized a series of 15−22-membered macrocyclic analogues of tripeptides and analyzed their structures. Each cycle is highly constrained by two trans amide bonds and a planar aromatic ring with a short nonpeptidic linker between them. A measure of this ring strain is the restricted rotation of the component tyrosinyl aromatic ring (ΔG_{rot} 76.7 kJ mol^{-1} (16-membered ring), 46.1 kJ mol^{-1} (17-membered ring)) evidenced by variable temperature proton NMR spectra (DMF-d_7, 200−400 K). Unusually large amide coupling constants ($^3J_{NH-CH\alpha}$ 9−10 Hz) corresponding to large dihedral angles were detected in both protic and aprotic solvents for these macrocycles, consistent with a high degree of structure in solution. The temperature dependence of all amide NH chemical shifts ($\Delta\delta/T$ 7−12 ppb/deg) precluded the presence of transannular hydrogen bonds that define alternative turn structures. Whereas similar sized conventional cyclic peptides usually exist in solution as an equilibrium mixture of multiple conformers, these macrocycles adopt a well-defined β-strand structure even in water as revealed by 2-D NMR spectral data and by a structure calculation for the smallest (15-membered) and most constrained macrocycle. Macrocycles that are sufficiently constrained to exclusively adopt a β-strand-mimicking structure in water may be useful pre-organized and generic templates for the design of compounds that interfere with β-strand recognition in biology.

Introduction

The extended "saw tooth" conformation of a peptide, known as a β-strand and defined by $\phi = -120 \pm 20°$ and $\psi = +120 \pm 20°$, is becoming increasingly acknowledged as a key structural motif in biology.[1−5] It is the fundamental recognition element in polypeptides that bind to classes of proteins such as proteolytic enzymes,[1] MHC proteins,[2] and SRC kinases.[3] It is also reportedly the key aggregating unit that leads to formation of amyloid deposits thought to be pathogenic for dementia diseases such as prion disorders[4] and Alzheimer's disease.[5] In combination as β-sheets, β-strands are important structural scaffolds in proteins as well as key recognition elements for interactions with DNA.[6] Only short peptide segments (3−10 amino acids) mediate all these biomolecular recognition events, yet short peptides on their own rarely adopt well-defined structures in solution, and the β-strand peptide conformation in particular is not a stable structure in water.[7] Thus, an important goal is to lock small organic molecules into rigid strand-mimicking structures[8] that are pre-organized for binding to such proteins. Structural pre-organization for binding to a macromolecular receptor can be expected to reduce the entropy loss associated with conformational rearrangement of a ligand into the shape required for receptor binding. If rigid strand mimetics could be realized, they might be valuable

* To whom correspondence should be addressed. E-mail: d.fairlie@imb.uq.edu.au. Telephone: +61-733651268. Fax: +61-733651990.

(1) (a) Fairlie, D.; West, M.; Wong, A. *Curr. Med. Chem.* **1998**, *5*, 29 and references therein. (b) Tyndall, J.; Fairlie, D. P. *J. Mol. Recognit.* **1999**, *12*, 1−8. (c) Fairlie, D. P.; Tyndall, J. D. A.; Reid, R. C.; Wong, A. K.; Abbenante, G.; Scanlon, M. J.; March, D. R.; Bergman, D. A.; Chai, C. L. L.; Burkett, B. A. *J. Med. Chem.* **2000**, *43*, 1271−1281.

(2) (a) Stern, L. J.; Brown, J. H.; Jardetzky, T. S.; Gorga, J. C.; Urban, R. G.; Strominger, J. L.; Wiley, D. C. *Nature* **1994**, *368*, 215−21. (b) Stanfield, R. L.; Wilson, I. A. *Curr. Opin. Struct. Biol.* **1995**, *5*, 103−13. (c) Siligardi, G.; Drake, A. F. *Biopolymers* **1995**, *37*, 281−92.

(3) (a) Stanfield, R. L.; Wilson, I. A. *Curr. Opin. Struct. Biol.* **1995**, *5*, 103−13. (b) Barzik, M.; Carl, U. D.; Schubert, W. D.; Frank, R.; Wehland, J.; Heinz, D. W. *J. Mol. Biol.* **2001**, *309*, 155−69.

(4) (a) Collinge, J. *Annu. Rev. Neurosci.* **2001**, *24*, 519−50. (b) Prusiner, S. B. *Proc. Natl. Acad. Sci. U.S.A.* **1998**, *95*, 13363−83.

(5) (a) Harkany, T.; Abraham, I.; Konya, C.; Nyakas, C.; Zarandi, M.; Penke, B.; Luiten, P. G. *Rev. Neurosci.* **2000**, *11*, 329−82. (b) Antzutkin, O.; Balbach, J. L.; Leapman, R. D.; Rizzo, N. W.; Reed, J.; Tycko, R. *Proc. Natl. Acad. Sci. U.S.A.* **2000**, *97*, 13045−13050.

(6) (a) Raumann, B. E.; Rould, M. A.; Pabo, C. O.; Sauer, R. T. *Nature* **1994**, *367*, 754−7. (b) Kim, Y.; Geiger, J. H.; Hahn, S.; Sigler, P. B. *Nature* **1993**, *365*, 512−20.

(7) (a) Zimm, B.; Bragg, J. *J. Chem. Phys.* **1959**, *31*, 526. (b) Scholtz, A.; Baldwin, R. L. *Annu. Rev. Biophys. Biomol. Struct.* **1992**, *21*, 95.

(8) (a) Glenn, M. P.; Fairlie, D. P. *Mini Reviews in Medicinal Chemistry* **2002**, in press and references therein. (b) Abbenante, G.; March, D. R.; Bergman, D. A.; Hunt, P. A.; Garnham, B.; Dancer, R. J.; Martin, J. L.; Fairlie, D. P. *J. Am. Chem. Soc.* **1995**, *117*, 10220. (c) Reid, R. C.; Fairlie, D. P. In *Advances in Amino Acid Mimetics and Peptidomimetics*; Abell, A., Ed.; JAI press: Greenwich, CT, 1997; Vol. 1, pp 77−107. (d) Smith, A. B., III; Keenan, T. P.; Holcomb, R. C.; Sprengeler, P. A.; Guzman, M. C.; Wood, J. L.; Carroll, P. J.; Hirschmann, R. *J. Am. Chem. Soc.* **1992**, *114*, 10672. (e) Smith, A. B., III; Guzman, M. C.; Sprengeler, P. A.; Keenan, P. A.; Holcomb, R. C.; Wood, J. L.; Carroll, P. J.; Hirschmann, R. *J. Am. Chem. Soc.* **1994**, *116*, 9947.

Scheme 1

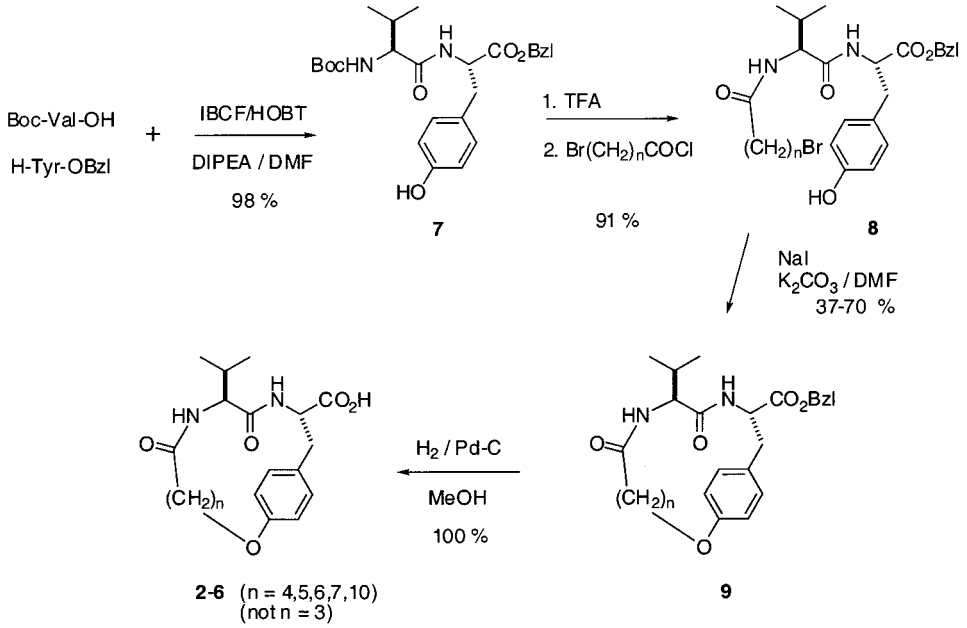

templates for mimicking these key recognition motifs, and, if sufficiently stable to biological degradation, they might find uses as molecular probes for recognition events associated with important biological processes or as drug leads for disease intervention.

One class of promising strand mimetics is macrocyclic peptidomimetics[1a,9,10] containing peptides or amino acids derivatized through side chain to side chain, side chain to main chain, or main chain to main chain linkages. The objective with macrocyclic peptidomimetics is to structurally mimic peptide binding to biological receptors with minimal disruption to the key protein-binding peptide components. Such macrocycles often have superior drug-like properties[1a,9,11] to acyclic peptides such as greater conformational integrity, enhanced stability to degradative enzymes, improved membrane permeability, and sometimes better oral activity. Although crystal structures have been reported by us and others for macrocyclic compounds bound to enzymes,[11,12] it was not known how accurately they mimic β-stranded peptides away from the enzyme-binding environment, and therefore to what extent they are pre-organized for receptor binding. In addition, many compounds have preferred structures in nonaqueous solvents, but it is not clear if that structure is retained in water. In this paper, we seek to address these matters by examining NMR spectral evidence for conformational rigidity of macrocycles **1**−**6**, constrained by two trans amide bonds, an aromatic ring originating from tyrosine, and an aliphatic linkage between tyrosine and valine.

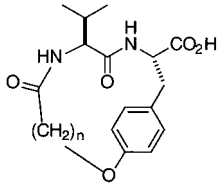

1-6 (n = 3,4,5,6,7,10)

Synthesis of Macrocyclic Acids. The dipeptide unit L-valinyl-L-tyrosine can be incorporated into macrocycles by alkylation of the tyrosine phenolic group and acylation of the valine amino terminus with a bifunctional bromoalkanoic acid. The order in which these steps are carried out can, as will be shown, affect the outcome of the reaction. Boc-Val-OH and H-Tyr-OBzl residues were coupled in solution with isobutyl chloroformate/HOBT giving the protected dipeptide (**7**), and then the Boc group was removed with TFA. Acylation of the N-terminus of the dipeptide with 5-bromopentanoyl chloride or the homologous C_{6-11}-bromoalkanoyl chlorides under Schotten−Baumann conditions proceeded rapidly to give (**8**) without complications from the free phenol. Formation of the macrocycle (**9**) under dilute conditions ($\leq$10 mM) was then effected (Scheme 1) by ring closure involving an ether linkage (Williamson) using anhydrous K_2CO_3 in DMF. Cleavage of the benzyl ester by hydrogenation (10% Pd/C) liberated the macrocyclic acids (**2**−**6**).

While this synthesis produces the larger macrocyclic acids (**2**−**6**) in up to 62% yield overall, the smaller macrocycles are compromised by competing intramolecular cyclization (Scheme 2) to the Val-amide nitrogen resulting either in contamination by the undesired δ-lactam (**10**) ($n = 4$), particularly following treatment with stronger bases such as potassium *tert*-butoxide, or in exclusive formation of the γ-lactam (**11**) ($n = 3$). In the latter case, the smallest 15-membered macrocycle (**1**) had to be prepared by a different ring closure, involving amide bond formation (Scheme 3).

Scheme 3 shows a synthesis in which the cyclization is effected through intramolecular amide bond formation but

(9) (a) Fairlie, D. P.; Abbenante, G.; March, D. R. *Curr. Med. Chem.* **1995**, *2*, 654 and references therein. (b) Scharn, D.; Germeroth, L.; Schneider-Mergener, J.; Wenschuh, H. *J. Org. Chem.* **2001**, *66*, 507.

(10) Tyndall, J. D. A.; Fairlie, D. P. *Curr. Med. Chem.* **2001**, *8*, 893−907 and references therein.

(11) Tyndall, J. D. A.; Reid, R. C.; Tyssen, D. P.; Jardine, D. K.; Todd, B.; Passmore, M.; March, D. R.; Pattenden, L. K.; Bergman, D. A.; Alewood, D.; Hu, S.-H.; Alewood, P. F.; Birch, C. J.; Martin, J. L.; Fairlie, D. P. *J. Med. Chem.* **2000**, *43*, 3495−3504.

(12) (a) Martin, J. L.; Begun, J.; Schindeler, A.; Wickramasinghe, W. A.; Alewood, D.; Alewood, P. F.; Bergman, D. A.; Brinkworth, R. I.; Abbenante, G.; March, D. R.; Reid, R. C.; Fairlie, D. P. *Biochemistry* **1999**, *38*, 7978−7988. (b) Smith, W. W.; Bartlett, P. A. *J. Am. Chem. Soc.* **1998**, *120*, 4622−4628. (c) Meyer, J. H.; Bartlett, P. A. *J. Am. Chem. Soc.* **1998**, *120*, 4600−4609.

Scheme 2

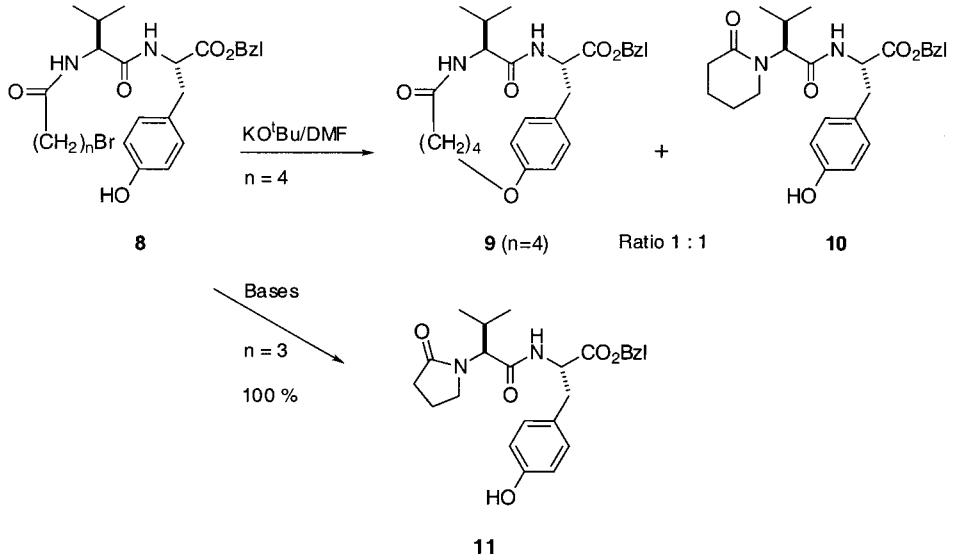

8 **9** (n=4) **10** **11**

Scheme 3

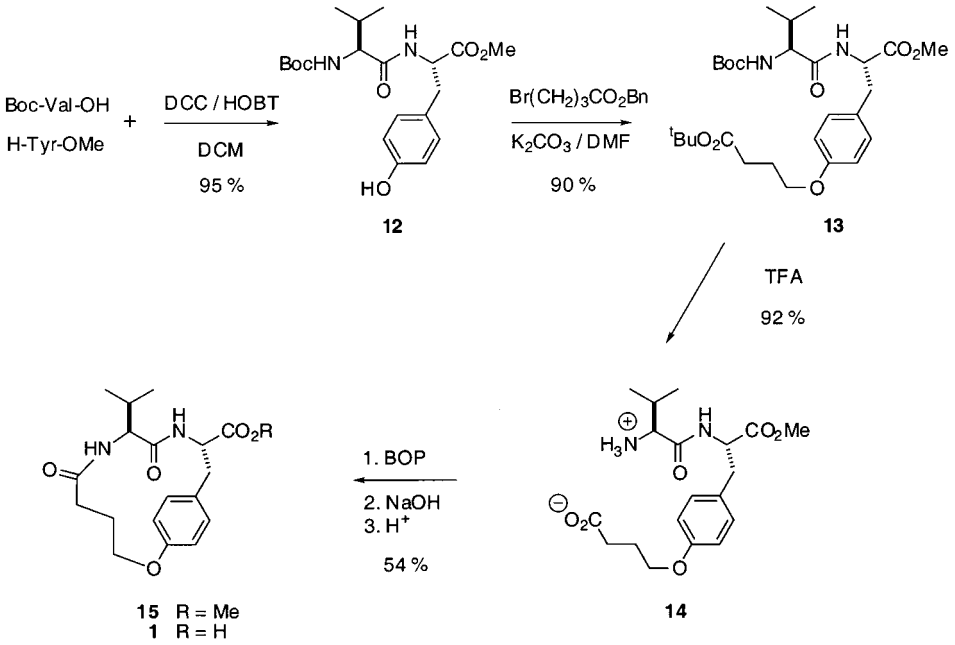

12 **13** **14** **15** R = Me **1** R = H

without the complication of γ- or δ-lactam side products. By this route, Boc-protected valine was coupled to tyrosine methyl ester giving the protected dipeptide (**12**), and the side chain phenol was alkylated with *tert*-butyl 4-bromobutyrate using anhydrous K_2CO_3 and NaI in DMF giving **13**. TFA treatment simultaneously removed *tert*-butyl ester and Boc groups giving the zwitterion (**14**) ready for cyclization. The zwitterion (**14**) was cyclized through amide bond formation using BOP reagent in dilute DMF solution. Hydrolysis of the methyl ester (**15**) gave the macrocyclic carboxylic acid (**1**).

Temperature-Dependent Ring Rotation. Figure 1 shows the temperature-dependent ^{1}H NMR spectra in the aromatic region for the macrocyclic acids **2** ($n = 4$) and **3** ($n = 5$) in DMF-d_7. At ambient temperature the aromatic ring gives rise to four resonances, one for each aromatic proton of the smaller 16-membered macrocycle **2**, but just two slightly broadened resonances typical of an AA′XX′ system for the aromatic ring protons of the 17-membered cycle **3**. This comparison reflects greater conformational restriction in the smaller macrocyclic ring of **2**, for which rotation of the aromatic ring on its 1,4 axis is slow on the NMR time scale, and unrestricted rotation only renders the protons chemically equivalent above 360 K (H_A, H_B, $\Delta\delta$ 70 Hz, $T_c = 380$ K; H_C, H_D, $\Delta\delta$ 36 Hz, $T_c = 360$ K; average $\Delta G^{\ddagger} = 76.7$ kJ mol^{-1}).

On the other hand, free rotation is observed by NMR spectroscopy for the aromatic ring of **3** above 230 K (H_A, H_B, $\Delta\delta$ 76 Hz, $T_c = 230$ K; H_C, H_D, $\Delta\delta$ 121 Hz, $T_c = 235$ K; average $\Delta G^{\ddagger} = 46.1$ kJ mol^{-1}). The free energy difference ($\Delta G^{\ddagger}$), calculated using the relationship[13] $\Delta G^{\ddagger} = RT_c[22.96 + \ln(T_c/\Delta\upsilon)]$, where T_c is the coalescence temperature for ortho- or meta-aromatic protons, and $\Delta\upsilon$ is the chemical shift difference (Hz), of 31 kJ mol^{-1} reflects the difference in rotational freedom between the aromatic rings of the two macrocycles. The smaller 15-membered ring in **1** does not show any sign of coalescence

(13) (a) Gunther, H. *NMR Spectroscopy: Basic Principles, Concepts, and Applications in Chemistry*, 2nd ed.; Wiley: Chichester, Brisbane, 1995. (b) Sandstrom, J. *Dynamic NMR Spectroscopy*; Academic Press: London, New York, 1982.

of the four aromatic ring proton resonances at 400 K, our limit for heating and thus detection, indicative of a much higher energy barrier to rotation.

Intramolecular Hydrogen Bonds. The conformational restriction observed above could theoretically result from intramolecular hydrogen bonding, such as between the Tyr-NH and the alkanoyl-CO defining a putative seven-membered ring typical of a γ-turn (e.g., **2a**). To assess whether the amide protons of the cycle **2** were intramolecularly hydrogen bonded, we first examined their exchange rates with deuterium. Slow amide H/D exchange is usually indicative of protection from solvent exposure, which can arise through steric protection or possibly from the presence of a hydrogen bond. The ^{1}H NMR resonance due to the Val-NH (δ 7.47 ppm, doublet, CD_3OD) is completely exchanged within 4−5 min at 22 °C, whereas the Tyr-NH (δ 8.35 ppm, doublet, CD_3OD) exchanges much more slowly and is still detectable after 1 h, consistent with a greater degree of solvent protection that might arise from transannular hydrogen-bonding (e.g., as in **2a**). Different relative rates of deuterium exchange were observed for all the macrocycles (**1**−**6**). Interestingly, a macrocyclic analogue of (**2**), containing arginine in place of valine, also showed slow exchange of the Tyr-NH. This suggests that shielding of the Tyr-NH from solvent was not solely related to the presence of the more hindering β-branched amino acid, but rather was due to the combined presence of amino acid side chains on both sides of the Tyr-NH.

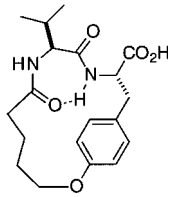

2a

Temperature Dependence of Amide NH Chemical Shifts. The temperature dependence of the amide NH chemical shifts was also examined for compounds **2** ($\Delta\delta/T$ = 7 ppb/deg (Tyr-NH), 8 ppb/deg (Val-NH)) and **3** ($\Delta\delta/T$ = 8 ppb/deg (Tyr-NH), 12 ppb/deg (Val-NH)) in DMF-d_7. This substantial temperature dependence is inconsistent with hydrogen-bonded amide NH protons which are normally temperature independent ($\Delta\delta/T$ < 4 ppb/deg).[14] Furthermore, the similarity of the $^3J_{NHCH\alpha}$ amide coupling constants for Val-NH and Tyr-NH, which are very large and characteristic of an extended β-strand, argues strongly against the involvement of the Tyr-NH in a transannular H-bond (e.g., **2a**). Therefore, it is very clear that the difference in deuterium exchange rates must originate from solvent protection of the Tyr-NH by amino acid side chains on either side (see Figure 3c ahead). It is quite common for H/D exchange rates to be slow even in the absence of H-bonds. There is similarly no intramolecular transannular hydrogen bonding for the macrocycles **1**−**3** when bound to HIV-1 protease as suggested by their X-ray crystal structures, since the amide nitrogens of the cycles are observed to be within appropriate distances and angles to constitute intermolecular hydrogen bonding with enzyme residues.[12]

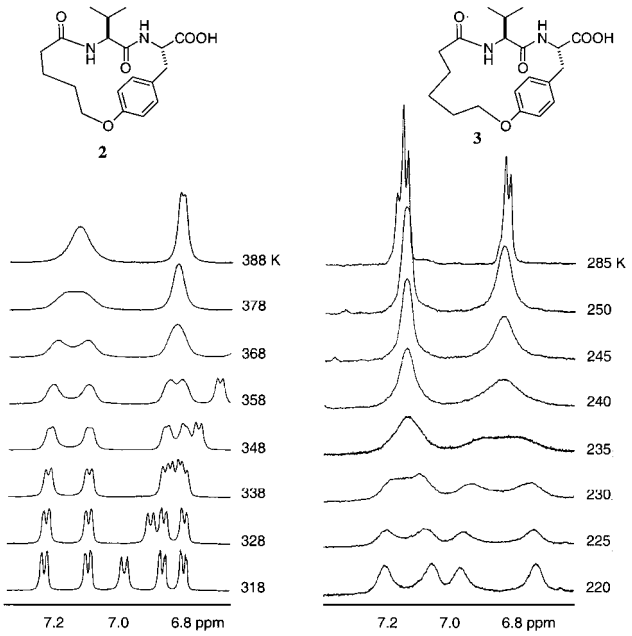

Figure 1. 500 MHz variable temperature ^{1}H NMR spectra of the aromatic regions of the conformationally constrained macrocyclic acids **2** (left) and **3** (right) in DMF-d_7 at 200−400 K. Energy barriers ($\Delta G^{\ddagger}$) to ring rotation for **2** (H_A, H_B, $\Delta\delta$ 70 Hz, T_c = 380 K; H_C, H_D, $\Delta\delta$ 36 Hz, T_c = 360 K) = 76.7 kJ mol^{-1}; for **3** (H_A, H_B, $\Delta\delta$ 76 Hz, T_c = 230 K; H_C, H_D, $\Delta\delta$ 121 Hz, T_c = 235 K) = 46.1 kJ mol^{-1}.

Estimation of ϕ Angles from Coupling Constants. The conformation of a peptide is determined by three repeating dihedral angles (ϕ, ψ, and ω) along the amide backbone. Peptides that adopt strand conformations can subsequently assemble into β-sheet structures for which the range of observed dihedral angles has largely been shown to be $\phi = -110$ to $-140°$ and $\psi = +110$ to $+135°$ from numerous high resolution X-ray crystal structures in the protein data bank (pdb). The calculated sterically allowed β-strand conformations defined in the β-region of the Ramachandran plot also confirm these dihedral angle ranges. Because the amide bond is comprised of sp^2 hybridized atoms, the dihedral ω is close to 180°.[15] An estimation of the angle ϕ can be made from the proton dihedral angle that is related to the $^3J_{NH-CH\alpha}$ coupling constant by the Karplus equation ($^3J_{NH-CH\alpha} = 6.4\cos^2(\phi - 60) - 1.4\cos(\phi - 60) + 1.9$) as parametrized by Pardi et al.[16] Whereas unstructured peptides that rapidly interconvert between many conformations show an averaged coupling constant of about 7 Hz,[17] larger couplings >8.5 Hz are indicative of stabilized structure.[18]

The smallest and therefore most constrained macrocycle herein, the 15-membered ring compound **1**, displayed the largest coupling constant between the Tyr NH and α-CH protons of 9.9 Hz indicative of a ϕ angle of ca. −120°, characteristic of β-strand structure. As the size of the macrocycle was increased progressively from 15 to 21 atoms, the coupling constant decreased only slightly suggesting that the overall β-strand conformation was retained with minimal averaging with other

(14) (a) Kessler, H. *Angew. Chem., Int. Ed. Engl.* **1982**, *21*, 512. (b) Llinas, M.; Klein, M. P. *J. Am. Chem. Soc.* **1975**, *97*, 4731−4737.

(15) (a) Brändén, C., Tooze, J. *Introduction to Protein Structure*, 2nd ed.; Garland: New York, 1999. (b) Karplus, P. A. *Protein Sci.* **1996**, *5*, 1406−1420.

(16) Pardi, A.; Billeter, M.; Wuthrich, K. *J. Mol. Biol.* **1984**, *180*, 741−51.

(17) (a) Griffiths-Jones, S. R.; Sharman, G. J.; Maynard, A. J.; Searle, M. S. *J. Mol. Biol.* **1998**, *284*, 1597−609. (b) Serrano, L. *J. Mol. Biol.* **1995**, *254*, 322−33.

(18) Mierke, D. F.; Huber, T.; Kessler, H. *J. Comput.-Aided Mol. Des.* **1994**, *8*, 29−40.

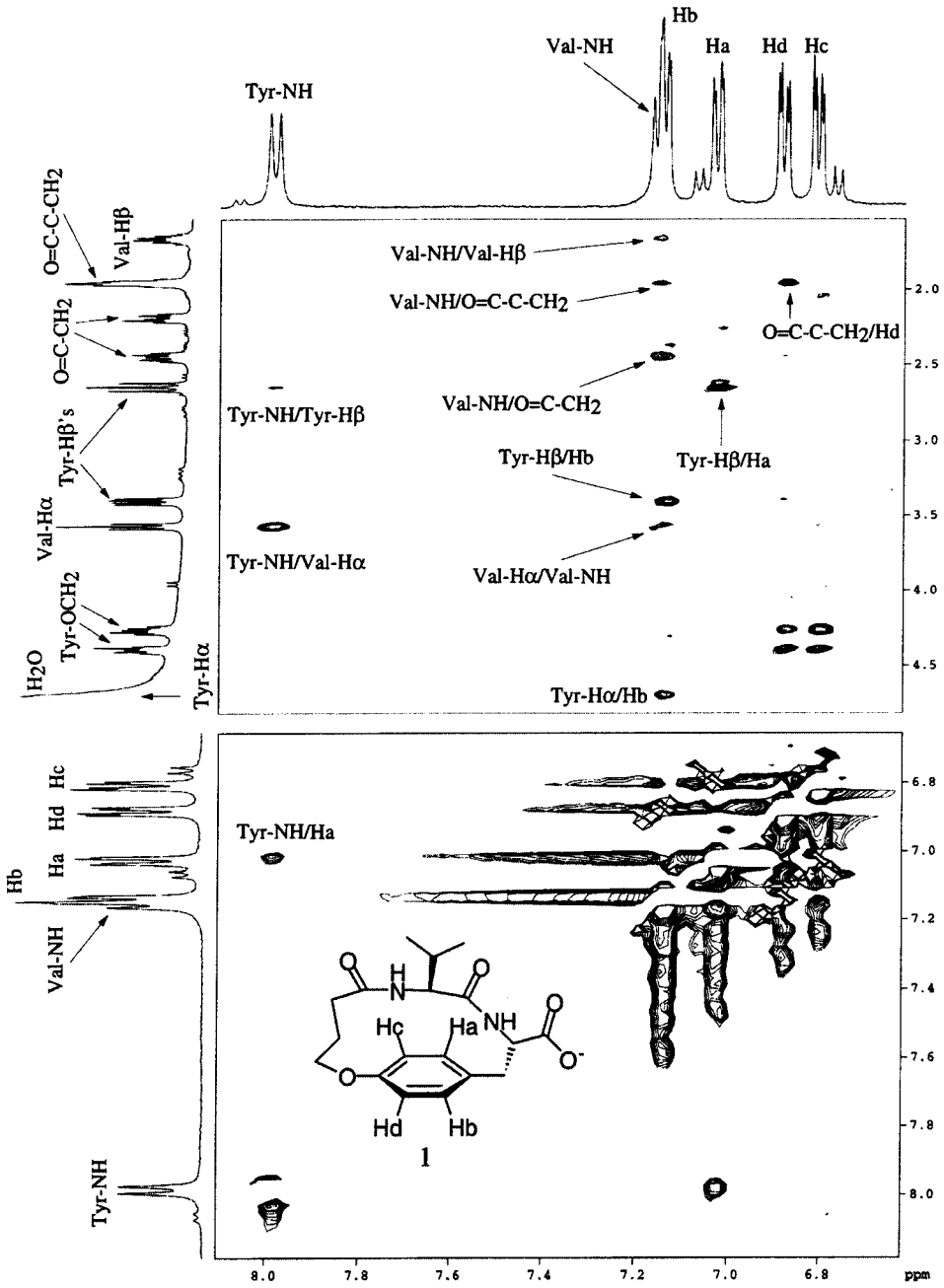

Figure 2. Sections of the 2-D-ROESY spectrum (400 ms) for **1**. 1-D projections are shown along the axes and include peak assignments. Unassigned peaks in the 1-D projections correspond to a small amount of a diketopiperazine (Supporting Information). The 11 ROE cross-peaks used as distance constraints for calculating the 3-D solution structure of **1** are labeled within the 2-D spectrum.

conformations. The valine residues of all macrocycles displayed nearly identical coupling constants between NH and α-CH protons of 9.2 ± 0.1 Hz corresponding to a ϕ angle of −105°, again demonstrating that all these macrocycles adopt conformationally stabilized β-strand structures.

Monte Carlo Conformational Searches for 1. Deriving NMR structures for cyclic peptides can be difficult due to the fact that cyclic peptides usually exist as mixtures of rapidly interconverting conformers in solution. Each of the conformational parameters measured by NMR spectroscopy (i.e., $^3J_{NH-CH\alpha}$ coupling constants, NOE data, etc.) represents an average structure that is dependent upon the number of conformers present in solution and their respective statistical weighting. Consequently, attempts to fit measured NMR parameters to a single three-dimensional structure are usually only justified for the most conformationally rigid of cyclic peptides, where a single conformer has a high predominance in solution.[19]

The ^{1}H NMR spectrum for **1** (Figure 2) was unusual in that it showed four discrete signals for each of the Tyr aromatic protons, indicating that its aromatic ring had been fixed into a particular conformation and that it was not free to rotate. This observation suggested that **1** is more conformationally rigid than typical cyclic peptides and that a calculated NMR structure may provide a reasonable picture of its predominant solution conformation(s).

(19) Nikiforovich, G. V.; Kövér, K. E.; Zhang, W.-J.; Marshall, G. R. *J. Am. Chem. Soc.* **2000**, *122*, 3262−3273.

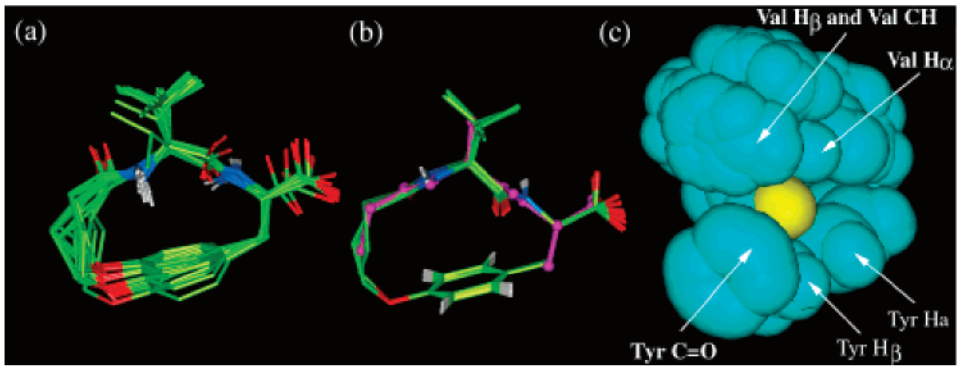

Figure 3. (a) Superimpositon of the 44 conformations of **1** generated by Monte Carlo simulation. (b) NMR solution structures of **1** in 90% H_2O:10% D_2O showing the superimposition of the 30 lowest energy conformations. Shown in purple in ball-and-stick representation is a theoretical β-strand (ϕ and ψ angles $-120°$ and $+120°$, respectively) superimposed on the solution structures of **1**, which clearly indicates that **1** is a tripeptide β-strand that deviates little from a theoretical or idealized β-strand. (c) Space-filling representation of (b) showing the degree of sterically hindrance of the Tyr−NH (yellow), and this can account for its slow H−D exchange behavior.

To validate this hypothesis, we submitted **1** to a preliminary round of Monte Carlo conformational searches and energy minimization protocols within the computer program Macromodel/BatchMin (version 7.0).[20] This technique provides a comprehensive insight into a molecule's inherent conformational variability, and we reasoned that if only a small number of conformers were identified by the search, then an NMR structure should be valid. The simulation carried out on **1** included a script to reject any structures that contained Val and Tyr residues with ϕ-dihedral angles not within $-140 < \phi < -100$, since it was known from ^{1}H NMR data ($^3J_{NH-CH\alpha}$ coupling constants) that these ϕ-angles were restricted to within this range. Inclusion of these types of constraints during Monte Carlo simulations has been shown to be a valuable technique for producing cyclic peptide structures that closely match their known solution structures.[21]

The simulations produced a set of only 44 unique macrocyclic ring conformations within 10 kcal/mol of the global energy minimum, reflecting a stark conformational rigidity for **1** despite having nine available torsions within the macrocycle. Indeed, all 44 conformers displayed very similar structures with the only significant variations being observed within the vicinity of the flexible $(CH_2)_3$ chain. This finding suggested that calculating an NMR solution structure for **1** was justified. The 44 conformations derived from the simulations are shown superimposed upon each other in Figure 3a.

NMR Structure for 1 in Water. Unambiguous assignment of most of the ^{1}H NMR resonances for **1** in 90% H_2O:10% D_2O was possible using a combination of 2-D-TOCSY,[22] DQF-COSY,[23] and ROESY[22,24] spectra. The methylene protons of the $(CH_2)_3$ chain were assignable with respect to their attached carbons but could not be stereospecifically assigned. The valine methyl groups were also unable to be stereospecifically assigned. The structures generated in the Monte Carlo simulations were used, in combination with data from 2-D ROESY spectra, as the basis for unambiguously assigning the individual Tyr aromatic protons (Ha, Hb, Hc, Hd) and also for stereospecifically assigning the Tyr Hβ-protons which were also defined unambiguously. As there were no detectable ROEs between Val CHα and Tyr CHα and between Val CHα and O=C−CH_2−, normally characteristic of cis peptide amide bonds, the presence of two trans amides was indicated.

The 2-D-ROESY spectrum (Figure 2) for **1** in 90% H_2O:10% D_2O contained 11 structurally relevant ROE correlations (Supporting Information, Table S1). We observed two H$\alpha(i)$-HN$(i+1)$ ROEs for dipeptide analogue **1**, O=C−CH_2 → Val-NH and ValHα → Tyr-NH, with medium intensity. These are typical of a β-strand, which is usually devoid of i, $i+1$ interresidue backbone ROEs. The H$\alpha(i)$-HN$(i+1)$ ROE (2.2 Å) is often the only ROE observed per residue, although a very weak HN(i)-HN$(i+1)$ NOE (4.3 Å) may sometimes be observed in a well-defined protein β-sheet.[25a] We did not see the latter for **1**. The observed intraresidue Val-Hα → Val-NH ROE was weaker than the interresidue Val-Hα → Tyr-NH ROE, and there was no Val NH → Tyr NH that would be expected to be present for a turn conformation. β-Strands are defined by three theoretical interrelated distances between H$\alpha(i)$, NH(i), and NH$(i+1)$ protons for each amino acid residue which are H$\alpha(i)$ → NH(i) = 3.0 Å, H$\alpha(i)$ → NH$(i+1)$ = 2.2 Å, NH$\alpha(i)$ → NH$(i+1)$ = 4.3 Å. The pattern of backbone ROEs we observed is consistent with these distances.

Another key indicator of β-structure is the presence of large coupling constants ($^3J_{NH-CH\alpha} \geq 8.5$ Hz) revealing $\phi \approx -120°$. We observed $^3J_{NH-CH\alpha}$ 9.2 Hz (Val), 9.9 Hz (Tyr) consistent with a β-strand. The Tyr coupling constant was extracted from a high digital resolution ^{1}H NMR spectrum, while the coupling constant for Val had to be extracted from a DQF-COSY spectrum since its NH signal was obscured by the Tyr Hb aromatic proton in the 1-D spectrum. The values of the ϕ-restraints used in structure calculations for **1** (Tyr $\phi = -120 \pm 20°$; Val $\phi = -120 \pm 20°$) were derived using the Karplus equation and are standard for structure calculations involving peptide-like molecules.[16,18]

The 3-D solution structure was calculated from the 11 ROE distance restraints and two backbone ϕ-dihedral angle restraints. The ROE intensities were classified by visual inspection as strong (upper distance constraint ≤2.7 Å), medium (≤3.5 Å), and weak (≤5.0 Å), and standard pseudoatom distance

(20) Mohamadi, F.; Richards, N. G. J.; Guida, W. C.; Liskamp, R.; Lipton, M.; Caufield, C.; Chang, G.; Hendrickson, T.; Still, W. C. *J. Comput. Chem.* **1990**, *11*, 440.
(21) Sefler, A. M.; Georges, L.; Bartlett, P. A. *Int. J. Pept. Protein Res.* **1996**, *48*, 129−138.
(22) Bax, A.; Davis, D. G. *J. Magn. Reson.* **1985**, *65*, 355−360.
(23) Derome, A.; Williamson, M. *J. Magn. Reson.* **1990**, *88*, 177−185.
(24) Hwang, T. L.; Shaka, A. J. *J. Am. Chem. Soc.* **1992**, *114*, 3157−3159.
(25) (a) Wüthrich, K.; Billeter, M.; Braun, W. *J. Mol. Biol.* **1984**, *180*, 715. (b) Wuthrich, K.; Billeter, M.; Braun, W. *J. Mol. Biol.* **1983**, *169*, 949.

corrections[25b] were added for nonstereospecifically assigned protons during structure calculations. The classifications were deliberately conservative, and only upper distance limits were included in the calculations to minimize the possibility of incorrectly biasing the structure.

The 3-D structures were calculated in XPLOR[30] using a dynamic simulated annealing protocol in a geometric force field and were energy minimized using a modified CHARMm[31] force field. The 30 lowest energy calculated structures are shown superimposed upon each other in Figure 3b. The calculated structures displayed low energies (0.8−3 kJ mol^{-1}) and had no residual distance violations greater than 0.2 Å or dihedral angle violations greater than 3° remaining. The backbone dihedral angles for each of the 30 structures were measured, and the averages were −100 ± 1° (Val ϕ), 138 ± 8° (Val ψ), −134 ± 5° (Tyr ϕ). Although these angles deviate from the theoretical (ϕ −120°, ψ +120°), they are within the variations normally observed in protein β-strands (vide supra). A single structural family was evident for **1** across the backbone atoms of Val and Tyr as well as Cβ and aromatic ring of Tyr. The aromatic ring of Tyr was clearly rigidified with minimal rotational freedom in close agreement with the 1-D NMR data. The only region of flexibility in **1** was within the $(CH_2)_3$ chain where two orientations of the chain satisfied the NMR restraints. Indeed the ROESY spectrum suggested that there may be two slowly interconverting orientations of this chain since both of the Tyr-O-CH_2 protons showed significant ROE cross-peaks to both the Hc and the Hd aromatic protons, an unlikely observation if only one conformation was present. Figure 3b shows that the solution conformation of **1** superimposes almost precisely upon the backbone and Cβ atoms of an idealized β-strand segment, showing that such macrocycles are highly optimized for β-strand mimicry.

Discussion

Numerous bioactive cyclic peptides containing structural restraints have been isolated from marine and terrestrial organisms, and many possess potentially useful medicinal properties, such as immunosuppressant, antiinflammatory, antitumor, antibacterial, and antiviral activities.[1−5,9,11] Even though certain nonpeptidic components are known to act as constraints by limiting conformational freedom in at least some macrocycles,[9,10] there have been surprisingly few detailed studies directed toward understanding how conformational constraints regulate three-dimensional structures of macrocycles in ways that influence reactivity.[9] There have, however, been many studies involving trial and error attempts to develop macrocycles to mimic the presumed protein-binding conformations of acyclic peptides.[11] Here we have used a minimalist approach to restrain a peptide into a β-strand conformation, employing amino acid side chain to backbone cyclization to fix conformation. We have demonstrated that this strategy successfully results in macrocycles such as **1** which structurally and functionally mimic tripeptide components of protease substrates and that their incorporation into larger molecules leads to subnanomolar inhibitors of at least one enzyme (HIV-1 protease).[9]

A key issue that we have not previously reported upon is the degree to which cycles such as **1**−**6** actually mimic a peptide β-strand prior to binding to a protein. We therefore synthesized a series of 15−22-membered macrocyclic analogues of tripeptides by condensing the tyrosinyl side chain of the dipeptide L-valinyl-L-tyrosine to its N-terminus using homologous bromoalkanoate linkers. Alkylation of the tyrosine phenolic group with a bifunctional bromoalkanoic acid followed by acylation of the valine amino terminus to close the macrocyclic ring was preferred for the smaller (15−16-membered) macrocycles over the reverse which was compromised by competing N-terminal lactam formation. The larger 17−22-membered macrocycles were prepared most efficiently by acylation first followed by ether formation to close the ring.

We have demonstrated herein that the smaller 15- and 16-membered macrocycles (**1**, **2**) are conformationally rigid molecules due to the presence of three regions of planarity (two amides, one aromatic ring) as well as a short aliphatic linker. While amides have a high barrier to rotation (∼70 kJ mol^{-1}) that preserves trans-amide stereochemistry, the aromatic ring in **1** and **2** is also sterically restricted from rotating about its 1,4-axis by the relatively small ring size in these macrocycles. This phenomenon was investigated by variable temperature ^{1}H NMR studies, and the barriers to rotation of the aromatic ring have been calculated for the different size macrocycles. Additional evidence of conformational rigidity in the macrocycles was provided by amide coupling constants, H−D exchange experiments, molecular modeling, and molecular dynamics techniques.

In particular, since water is the solvent in which a peptide exists prior to binding in the active site of a protein, we particularly wanted to identify the solution structure of a strand mimetic in water. The three-dimensional solution structure was determined for the smallest and most constrained cycle (**1**) in water. The highly constrained structure observed for **1** was a predominantly β-strand-mimicking conformation. It is interesting to note that the unusually high amide coupling constants ($^3J_{NH-CH\alpha}$) observed for the two backbone amides were very similar in water, DMF, DMSO, MeOH, and $CDCl_3$ (some data not shown), suggesting that the β-strand conformation of **1** is highly conserved in all of these solvents.

A desirable feature of a β-strand mimetic is that it has hydrogen bond donors/acceptors free to interact with a receptor. Clearly this means that there should be no intramolecular hydrogen bonds in the mimetic prior to receptor binding, since these would need to be broken before complexation. Although the VT-NMR experiments above suggested that the amide NH protons in **2** and **3** were temperature dependent and therefore were unlikely to be participating in H-bonding, the H/D exchange data suggested that the Tyr-NH was unusually slow to exchange. It became clear following structure determination of **1** that this is due to steric protection from solvent exposure. However, this was not due to the valine side chain, since arginine at this position showed similar behavior, but rather is due to steric crowding from the aromatic ring and CHα of Val/

(26) Still, W. C.; Tempczyk, A.; Hawly, R. C.; Hendrickson, T.; Still, W. C. *J. Am. Chem. Soc.* **1990**, *112*, 6127.
(27) The calculated structures were read into Insight II Version 2000 (Molecular Simulations Inc. (Accelrys), San Diego, CA) as.pdb files for visualization and display.
(28) Marion, D.; Wuthrich, K. *Biochem. Biophys. Res. Commun.* **1983**, *113*, 967.
(29) Nilges, M.; Gronenborn, A. M.; Brünger, A. T.; Clore, G. M. *Protein Eng.* **1988**, *2*, 27.
(30) Brünger, A. T. *X-PLOR Manual Version 3.1*, Yale University, New Haven, CT, 1992.
(31) Brooks, B. R.; Bruccoleri, R. E.; Olafson, B. D.; States, D. J.; Swaminathan, S.; Karplus, M. *J. Comput. Chem.* **1983**, *4*, 187.

Arg (Figure 3c). Thus we conclude that intramolecular H-bonding to form β or γ turns is specifically prevented due to the highly restrained conformation of **1**−**6**.

The use of conformationally constrained macrocycles such as **1** is dependent of appropriate synthetic methods that enable their construction in reasonable quantities and allow ready incorporation of nonpeptidic appendages. We herein report versatile and simple synthetic routes to these macrocycles suitable for scale-up syntheses. The macrocycles offer a number of advantages over the acyclic peptides which they mimic, including conformational restriction that confers structural homogeneity, stability toward peptide bond cleavage by degradative proteolytic enzymes,[1a,8−11] removal of peptide zwitterionic character, and increased lipophilicity. This work suggests that other conformationally constrained cyclic peptides with alternative constraints could similarly fix a β-strand-mimicking structure, and such molecules may find further uses as components of protease inhibitors, SRC kinase inhibitors, MHC-binding inhibitors, and in agents for the prevention or treatment of amyloidogenic and other diseases involving aggregating or receptor-binding β-strands.

Experimental Section

Monte Carlo Conformational Searches for 1. Monte Carlo simulations and energy minimizations for **1** were carried out using Macromodel/BatchMin software (version 7.0).[20] The searches were performed with 10 000 iterations in which all of the amide bonds were set to trans, and chirality checking (CHIG) was employed to ensure the stereochemical integrity of the Val and Tyr α-carbons. A minimum of two and a maximum of nine torsions were altered in each Monte Carlo step, and the resulting conformers were minimized to gradient convergence according to the PR conjugate gradient (PRCG)-type minimization protocol within a GB/SA water solvation model.[26] Structures that contained Val and Tyr ϕ-dihedral angles outside of the range $-140 < \phi < -100$ were automatically rejected. The search yielded only 44 unique conformations, all of which were found multiple times indicating that the conformational space had been explored adequately and that **1** is highly constrained.[20]

2-D-NMR Spectroscopy. The sample used for NMR measurements was obtained by adding 90% H_2O:10% D_2O (v/v) (600 μL) to 3.0 mg (8.6 μmol; concentrated = 14.4 mM) of **1** in an NMR tube followed by 0.72 mg (8.6 μmol, 1 equiv) of $NaHCO_3$ to produce the water-soluble sodium salt. 2-D-NMR spectra were recorded at 293 K in phase-sensitive mode using time-proportional phase incrementation for quadrature detection in the t_1 dimension[28] on a Bruker DRX-500 spectrometer. COSY spectra were obtained using the standard Bruker pulse program cosydfprtp with 512 increments in F1 and 8 K data points in F2 with 16 scans per increment. TOCSY spectra were obtained using the pulse program mlevprtp with 80 ms mixing time, 512 F1 increments (8 scans each), and 2 K data points in F2. ROESY spectra were acquired using the pulse program roesyprtp with mixing times of 250 ms and 400 ms. In F1, 1024 increments were acquired, with 4 K data points in F2 and 16 scans per increment. No differences were observed in the two ROESY spectra for **1** with different mixing times. Solvent suppression was achieved for all spectra in water using a low power presaturation pulse. A sweep width of 4762 Hz was employed for all acquisitions. 2-D spectra were processed using XWINNMR (Bruker, Germany). In all cases, the t_1 dimension was zero-filled to 2048 real data points, and 90° phase-shifted sine bell window functions applied in both dimensions followed by Fourier transformation and fifth order polynomial baseline correction.

Solution Structure Calculation. ROE cross-peak intensities from the 400 ms ROESY spectrum of **1** in 90% H_2O:10% D_2O were classified by visual inspection as strong (upper limit for internuclear distance restraint ≤2.7 Å), medium (≤3.5 Å), or weak (≤5.0 Å). Starting structures with randomized ϕ and ψ angles and extended side chains were generated for **1** using an ab initio simulated annealing protocol.[29] Preliminary structures were then calculated from a combination of the ROESY data (no lower limits for distances were employed in the calculations) and ϕ-angle coupling constant data using a dynamic simulated annealing and energy minimization protocol in the program XPLOR[30] (version 3.851). The preliminary structures were refined to produce the final ensemble using the conjugate gradient Powell algorithm with 1000 cycles of energy minimization and a refined force field based on the program CHARMm.[31] The backbone dihedral angle restraints employed during the calculations were inferred from $^3J_{NH-CH\alpha}$ coupling constants (measured from high digital resolution ^{1}H spectra in the case of Tyr and DQF-COSY spectra in the case of Val) with both ϕ-angles being restrained to $-120 \pm 20°$. Peptide bond ω angles were all set to trans. Structures were displayed using Insight II (Version 2000, Molecular Simulations Inc. (Accelrys), San Diego, CA).

Only upper distance constraints were used in the structure calculations, and the constraints derived from ROE intensities were purposely conservative, to prevent biasing of the structure toward conformations that are not satisfied by the NMR data and to diminish the effects of experimental inaccuracies in ROE intensities. In a highly constrained molecule like **1**, this approach is valid because even with no distance restraints, only β-strand conformations very similar to the NMR structure were found (Figure 3a). The effects of adding the ROE derived distance constraints simply aided convergence to the structure shown in Figure 3b.

Chemical Synthesis. General Considerations. All amino acid derivatives were obtained from Calbiochem-Novabiochem and were used as received. DMF, TFA, DIPEA, DCC, HOBT, and BOP were "peptide synthesis grade" reagents obtained from Auspep Pty. Ltd. Australia. Reverse phase HPLC was carried out on Phenomenex Luna C18 columns 250 × 4.6 mm analytical or 250 × 22 mm preparative at flow rates of 1 and 20 mL min^{-1}, respectively, with detection at 276 nm. NMR spectra were referenced to the residual solvent peaks $CDCl_3$ δ_H 7.27, δ_C 77.0 ppm; DMSO δ_H 2.49, δ_C 39.5 ppm; CD_3OD δ_C 49.0 ppm or TMS if present. High-resolution mass spectra were recorded on a Finnigan 2000 Fourier transform spectrometer (3 T) with resolving power greater than 20 000. Nomenclature was suggested by the computer program "Beilstein AutoNom V2.1" within ChemDraw V6.0.

Boc-Val-Tyr-OBzl (7). Boc-Val-OH (16.98 g, 78.2 mmol) was dissolved in THF (250 mL), and *N*-methyl morpholine (9 mL, 81.6 mmol, 1.04 equiv) was added. The solution was stirred at −15 °C under argon, and then isobutyl chloroformate (10.5 mL, 80.9 mmol) was added in 10 portions over 10 min at −10 °C. After a further 5 min, HOBT (10.8 g, 80 mmol) was added, and the mixture was warmed to 0 °C. H-Tyr-OBzl·TsOH (36 g, 78 mmol) was added followed by DCM (100 mL) and *N*-methyl morpholine (9 mL), and the mixture was stirred at room temperature for 3 h. The solution was washed with 2 M HCl, 1 M $NaHCO_3$ twice, and dried over $MgSO_4$. Removal of solvent gave a white solid (36 g, 98%) R_f 0.54 (50% EtOAc/petrol). ^{1}H NMR (300 MHz, $CDCl_3$): δ 7.41−7.27 (m, 5H), 6.83 (d, J = 8.3 Hz, 2H), 6.65 (d, J = 8.3 Hz, 2H), 6.46 (d, J = 8.0 Hz, 1H), 5.18 and 5.11 (AB quartet, J_{AB} = 12.1 Hz, 2H), 5.11 (m, NH overlapped 1H), 4.88 (m, 1H), 3.87 (m, 1H), 3.07−2.97 (m, 2H), 2.03 (m, 1H), 1.45 (s, 9H), 0.89 (d, J = 6.8 Hz, 3H), 0.85 (br d, J = 6.6 Hz, 3H).

6-Bromohexanoyl-L-valinyl-L-tyrosine Benzyl Ester (8, n = 5). Boc-Val-Tyr-OBzl (**7**) (4.80 g, 10.2 mmol) was dissolved in neat TFA, and then after 15 min was evaporated to dryness in vacuo. The residue was dissolved in THF (30 mL) and water (30 mL) and was stirred at room temperature while solutions of 6-bromohexanoyl chloride (2.4 g, 11 mmol) in THF (5 mL) and 20% K_2CO_3 (10 mL) were added together maintaining pH 9. After 30 min, the mixture was diluted with EtOAc and washed with 2 M HCl, 5% $NaHCO_3$, brine, and dried over $MgSO_4$. Removal of solvent gave a white solid (5.1 g, 91%) mp 140−143 °C. R_f 0.68 (100% EtOAc), R_f 0.23 (50% EtOAc/hexane). ^{1}H NMR

(300 MHz, $CDCl_3$): δ 7.42−7.25 (m, 5H, Ph), AA′XX′ system, 6.82 (m, 2H, $J_{AX} + J_{AX'} = 8.5$ Hz, ortho to CH_2), 6.66 (m, 2H, $J_{AX} + J_{AX'} = 8.5$ Hz, ortho to O), 6.57 (d, $J = 7.9$ Hz, 1H, Tyr-NH), 6.31 (d, $J = 8.9$ Hz, 1H, Val-NH), AB system (δ_A 5.20, δ_B 5.12, $J_{AB} = 12.0$ Hz, OCH_2Ph), 4.88 (m, 1H, Tyr-αCH), 4.28 (dd, $J = 8.8$, 7.1 Hz, 1H, Val-αCH), 3.39 (apparent t, $J = 6.7$ Hz, 2H, CH_2Br), 3.10−2.93 (m, 2H, Tyr-βCH_2), 2.29−2.19 (m, 2H, CH_2CO), 2.00 (m, 1H, Val-βCH), 1.91−1.40 (m, 6H, $(CH_2)_3$), 0.89 (d, $J = 6.7$ Hz, Val-γCH_3), 0.88 (d, $J = 6.7$ Hz, Val-γCH_3). ^{13}C NMR ($CDCl_3$): δ 173.2, 171.0, 155.5, 135.0, 130.4, 128.6, 126.6, 115.6, 67.4, 58.3, 53.3, 36.9, 36.3, 33.6, 32.3, 31.2, 27.7, 24.8, 19.0, 18.2. HRMS *m*/*e* 546.1731, M^+ calc. for $C_{27}H_{35}N_2O_5{}^{79}$Br 546.1729.

5-Bromopentanoyl-L-valinyl-L-tyrosine Benzyl Ester (8, *n* = 4). This was prepared by the procedure for **8** ($n = 5$) using 5-bromopentanoyl chloride in 95% yield. ^{13}C NMR ($CDCl_3$): δ 172.9, 171.1, 171.0, 155.4, 135.0, 130.4, 128.6, 126.7, 115.6, 67.4, 58.3, 53.3, 36.9, 35.4, 33.1, 32.0, 31.2, 24.2, 19.1, 18.2. HRMS *m*/*e* 555.1462, MNa^+ calc. for $C_{26}H_{33}N_2O_5{}^{79}$BrNa 555.1465.

4-Bromobutyryl-L-valinyl-L-tyrosine Benzyl Ester (8, *n* = 3). This was prepared by the procedure for **8** ($n = 5$) using 4-bromobutyryl chloride in 95% yield R_f 0.74 (100% EtOAc).

Anal. Calcd for $C_{25}H_{31}N_2O_5Br$: C, 57.81; H, 6.02; N, 5.39. Found: C, 57.49; H, 6.21; N, 5.31. ^{1}H NMR (300 MHz, $CDCl_3$ + d_6-DMSO 10%): δ 7.41−7.23 (m, 5H), 7.06 (d, $J = 8.9$ Hz, 1H), 6.90 (d, $J = 8.4$ Hz, 2H), 6.70 (d, $J = 8.4$ Hz, 2H), 5.10 (s, 2H), 4.76 (m, 1H), 4.27 (dd, $J = 8.8$, 6.9 Hz, 1H), 3.46 (t, $J = 6.6$ Hz, 2H), 3.08−2.92 (m, 2H), 2.43−2.34 (m, 2H), 2.22−2.09 (m, 2H), 2.05 (m, 1H), 0.92−0.84 (m, 6H).

10*S*-Isopropyl-8,11-dioxo-2-oxa-9,12-diaza-bicyclo[13.2.2]nonadeca-1(18),15(19),16-triene-13*S*-carboxylic Acid Benzyl Ester (9, *n* = 5). A solution of the bromide (**8**, $n = 5$) (902 mg, 1.65 mmol) and NaI (500 mg) in acetone (10 mL) was stirred at room temperature overnight, and then evaporated. The residue was dissolved in EtOAc and washed with brine, dried over $MgSO_4$, and evaporated to dryness to give the corresponding iodide (HRMS *m*/*e* 617.1486, MNa^+ calc. for $C_{27}H_{35}N_2O_5$-INa 617.1483). The residual iodide was dissolved in dry DMF (100 mL), and finely ground anhydrous K_2CO_3 (1.05 g) was added. The mixture was stirred at room temperature overnight, and then concentrated in vacuo. The residue was dissolved in $CHCl_3$/EtOAc (1:1) and washed with water, brine, and dried over $MgSO_4$. Removal of solvent gave the macrocycle as a white solid (580 mg, 70%). R_f 0.35 (50% EtOAc/$CHCl_3$). ^{1}H NMR (300 MHz, $CDCl_3$): δ 7.45−7.30 (m, 5H, Ph), 7.03 (m, 2H, meta to O), 6.82 (m, 2H, ortho to O), 5.88 (m, 2H, NH and NH), AB system (δ_A 5.27, δ_B 5.19, $J_{AB} = 12.1$ Hz, OCH_2Ph), 5.04 (ddd, $J = 12.2$, 9.6, 4.6 Hz, Tyr-αH), 4.30−4.11 (m, 2H, H-3), 4.01 (dd, $J = 8.6$, 6.6 Hz, 1H, Val-αH), 3.41 (dd, $J = 13.9$, 4.6 Hz, 1H, Tyr-βH), 2.56 (dd, $J = 13.9$, 12.2 Hz, 1H, Tyr-βH), 2.25−2.19 (m, 1H, CH_2CO), 2.15−1.10 (e), 0.85 (d, $J = 6.8$ Hz, 3H, Val-γ CH_3), 0.84 (d, $J = 6.8$ Hz, 3H, Val-γ CH_3). ^{13}C NMR ($CDCl_3$): δ 171.8, 171.3, 170.2, 157.5, 130.2, 128.7, 128.6, 128.5, 127.7, 116.4, 67.4, 67.5, 57.7, 52.5, 38.0, 35.6, 31.9, 29.2, 25.1, 24.6, 18.7, 18.3.

9*S*-Isopropyl-7,10-dioxo-2-oxa-8,11-diaza-bicyclo[12.2.2]octadeca-1(17),14(18),15-triene-12*S*-carboxylic Acid Benzyl Ester (9, *n* = 4). The bromide (**8**, $n = 4$) (935 mg, 1.75 mmol) was converted to the corresponding iodide by refluxing with NaI (395 mg) in acetone (20 mL) for 2 h, then the precipitated NaCl was filtered off, and the solvent was evaporated. The residual iodide was dissolved in dry DMF (50 mL), and anhydrous K_2CO_3 (500 mg) was added. The mixture was stirred at room temperature overnight, and then evaporated in vacuo. The residue was partitioned between water and 50% EtOAc/$CHCl_3$, and the organic layer was filtered to remove solid polymer, then washed with dilute sodium thiosulfate solution, 2 M HCl, $NaHCO_3$, and dried over $MgSO_4$. Removal of solvent gave a solid which was purified by flash chromatography ($CHCl_3$ − 50% EtOAc/$CHCl_3$) giving a white powder (290 mg, 37%). R_f 0.28 (75% EtOAc/hexane). ^{1}H NMR (300 MHz, $CDCl_3$): δ 7.45−7.35 (m, 5H, ArH), 7.21 (dd, $J = 8.4$, 2.2 Hz, 1H, ArH), 6.92−6.84 (m, 2H, ArH), 6.78 (dd, $J = 8.3$, 2.7 Hz, 1H, ArH), 5.83 (d, $J = 9.9$ Hz, 1H, tyr NH), 5.69 (d, $J = 8.8$ Hz, 1H, val NH), AB system, δ_A 5.26, δ_B 5.20, $J_{AB} = 13.1$ Hz, 2H, OCH_2Ph), 5.06 (ddd, $J = 14.9$, 10.0, 4.8 Hz, 1H, tyr αH), 4.29−4.12 (m, 2H, CH_2OAr), 3.95 (dd, $J = 8.8$, 7.1 Hz, 1H, val αH), 3.43 (dd, $J = 13.6$, 4.8 Hz, 1H, tyr βH), 2.53 (dd, $J = 13.6$, 12.1 Hz, 1H, tyr βH), 2.26−2.17 (m, 1H) and 2.09−1.98 (m, 1H, CH_2CO), 1.98−1.70 (m, 2H, CH_2), 1.83 (m, 1H, val βH), 1.55−1.31 (m, 2H, CH_2), 0.84 (d, $J = 6.8$ Hz, 6H, $(CH_3)_2$). ^{13}C NMR ($CDCl_3$): δ 172.07, 171.25, 170.02, 155.71, 135.04, 131.12, 129.99, 128.72, 128.69, 128.46, 128.34, 118.34, 116.52, 67.81, 67.49, 58.16, 52.48, 38.46, 36.12, 31.78, 25.98, 21.66, 18.77, 18.40. HRMS *m*/*e* 452.2312, M^+ calc. for $C_{26}H_{32}N_2O_5$ 452.2311.

3-(4-Hydroxy-phenyl)-2-[3-methyl-2-(2-oxo-piperidin-1-yl)-butyrylamino]-propionic Acid Benzyl Ester (10). A solution of the bromide (**8**, $n = 4$) (500 mg, 0.94 mmol) in THF (50 mL) was stirred at room temperature, and then KO^{t}Bu (110 mg, 0.98 mmol) was added. After 2 h, the solvent was evaporated, and the residue was analyzed by rp-HPLC which showed the δ-lactam (**10**) R_t 8.1 min and the macrocycle (**11**) R_t 7.8 min (54% MeCN, 46% H_2O, 0.1% TFA isocratic) in the ratio 98:2. An analytical sample of the δ-lactam was purified by preparative HPLC giving a white powder.

^{1}H NMR (300 MHz, $CDCl_3$): δ 7.41−7.31 (m, 5H), 6.87 (AA′XX′ system, $J_{AX} + J_{AX'} = 8.5$ Hz, 2H), 6.77 (d, $J = 7.7$ Hz, 1H), 6.68 (AA′XX′ system, JAX + JAX = 8.5 Hz, 2H), 5.22 and 5.13 (AB quartet, JAB = 12.2 Hz, 2H), 4.84 (m, 1H), 4.54 (d, $J = 11.3$ Hz, 1H, Val CH), 3.28−3.12 (m, 2H), 3.12 (dd, $J = 14.2$, 4.9 Hz, 1H), 2.90 (dd, $J = 14.2$, 8.0 Hz, 1H), 2.51−2.13 (m, 3H), 1.98−1.53 (m, 4H), 0.88 (d, $J = 6.4$ Hz, 3H), 0.80 (d, $J = 6.6$ Hz, 3H). ^{13}C NMR ($CDCl_3$): 171.6, 171.0, 169.4, 155.7, 135.2, 130.1, 128.6, 128.48, 128.46, 126.7, 115.5, 67.2, 62.7, 53.0, 43.4, 36.6, 32.0, 25.2, 22.8, 20.5, 19.5, 18.4. ISMS 453 (MH+).

3-(4-Hydroxy-phenyl)-2-[3-methyl-2-(2-oxo-pyrrolidin-1-yl)-butyrylamino]-propionic Acid Benzyl Ester (11). The bromide (**8**, $n = 3$) (52 mg, 0.10 mmol) and anhydrous K_2CO_3 (100 mg) were stirred in DMF (10 mL) at room temperature overnight. The solvent was evaporated, and the residue was dissolved in EtOAc and washed with water, brine, dried over $MgSO_4$, and evaporated to dryness. The residue (39 mg, 89%) was shown to be the γ-lactam, and no macrocycle was present. ^{1}H NMR (300 MHz, $CDCl_3$): δ 7.42−7.31 (m, 5H), 6.83 (AA′XX′ system, $J_{AX} + J_{AX'} = 8.5$ Hz, 2H), 6.71 (m, 1H, NH overlaps aromatics), 6.67 (AA′XX′ system, $J_{AX} + J_{AX'} = 8.5$ Hz, 2H), 5.24 and 5.14 (AB quartet $J_{AB} = 12.4$ Hz, 2H), 4.91 (m, 1H), 4.00 (d, $J = 11.1$ Hz, 1H), 3.39−3.25 (m, 2H), 3.12 (dd, $J = 14.1$, 5.0 Hz, 1H), 2.91 (dd, $J = 14.1$, 7.6 Hz, 1H), 2.52−2.32 (m, 2H), 2.24 (m, 1H), 2.01−1.88 (m, 2H), 0.88 (d, $J = 6.5$ Hz, 3H), 0.80 (d, $J = 6.6$ Hz, 3H). ISMS 439 (MH^+).

Boc-Val-Tyr-OMe (12). A solution of Boc-Val-OH (3.0 g 13.8 mmol), H-Tyr-OMe (2.7 g, 13.8 mmol), and HOBT (1.9 g, 13.8 mmol) in DCM (50 mL) was stirred at room temperature, and then DCC (2.8 g, 13.8 mmol) was added. The mixture was stirred for 4 h, and then the urea was filtered off. The filtrate was washed with 1 M HCl, 5% $NaHCO_3$, dried over $MgSO_4$, and evaporated to give a white solid (5.1 g, 95%). ^{1}H NMR (300 MHz, $CDCl_3$): δ 7.25 (s, 1H), 6.92 (d, $J = 8.3$ Hz, 2H), 6.70 (d, $J = 8.3$ Hz, 2H), 6.61 (d, $J = 7.7$ Hz, 1H), 5.18 (d, $J = 8.7$ Hz, 1H), 4.85 (m, 1H), 3.87 (m, 1H), 3.72 (s, 3H), 3.11−2.96 (m, 2H), 2.15−1.97 (m, 1H), 1.46 (s, 9H), 0.97−0.83 (m, 6H).

4-{4-[2-(2-*tert*-Butoxycarbonylamino-3-methyl-butyrylamino)-2-methoxycarbonyl-ethyl]-phenoxy}-butyric Acid *tert*-Butyl Ester (13). A solution of Boc-Val-Tyr-OMe (2.90 g, 7.36 mmol), *tert*-butyl 4-bromobutyrate (2.46 g, 11.0 mmol 1.5 equiv), NaI (1.1 g), and K_2CO_3 (2.0 g, 14.5 mmol) in dry DMF (8 mL) was stirred at 40 °C for 24 h. Volatiles were evaporated under high vacuum, and the residue was dissolved in EtOAc and washed with 1% sodium thiosulfate, 5% $NaHCO_3$, brine, and dried over $MgSO_4$. Flash chromatography (30−50% EtOAc/petrol) afforded a gum (3.54 g, 90%) R_f 0.50 (50% EtOAc/petrol). ^{1}H NMR (300 MHz, $CDCl_3$): δ 7.01 (d, $J = 8.5$ Hz,

2H), 6.80 (d, J = 8.5 Hz, 2H), 6.25 (d, J = 1H), 5.01 (d, J = 1H), 4.82 (m, 1H), 3.96 (t, J = 6.1 Hz, 2H), 3.89 (m, 1H), 3.71 (s, 3H), 3.10−3.02 (m, 2H), 2.42 (t, J = 7.4 Hz, 2H), 2.19−1.99 (m, 3H), 1.45 (s, 18H), 0.98−0.79 (m, 6H). ^{13}C NMR ($CDCl_3$): δ 172.4, 171.7, 171.2, 158.0, 155.6, 130.1, 127.5, 114.5, 80.2, 79.7, 66.7, 59.8, 53.2, 52.2, 37.0, 31.9, 30.8, 28.2, 28.0, 24.7, 19.1, 17.6. ISMS 537 (MH^+), 559 (MNa^+), 481, 437, 381.

4-{4-[2-(2-Amino-3-methyl-butyrylamino)-2-methoxycarbonyl-ethyl]-phenoxy} Butyric Acid (14). The protected dipeptide derivative (**13**) (380 mg, 0.71 mg) was dissolved in neat TFA (2 mL), and then after 15 min was evaporated. The residue was purified by rp-HPLC (22% MeCN, 78% H_2O, 0.1% TFA, R_t 9.5 min) giving a white powder (248 mg, 92%) after lyophilization. ^{1}H NMR (300 MHz, d_6-DMSO): δ 8.81 (d, J = 7.1 Hz, 1H), 8.06 (br s, 3H), 7.13 (d, J = 8.6 Hz, 2H), 6.83 (d, J = 8.6 Hz, 2H), 4.49 (m, 1H), 3.93 (t, J = 6.4 Hz, 2H), 3.63 (m, 1H), 3.59 (s, 3H), 2.98 (dd, J = 14.1, 5.8 Hz, 1H), 2.89 (dd, J = 14.1, 8.4 Hz, 1H), 2.36 (t, J = 7.1 Hz, 2H), 2.10 (m, 1H), 1.95−1.85 (m, 2H), 0.94 (d, J = 6.9 Hz, 3H), 0.90 (d, J = 6.9 Hz, 3H). ^{13}C NMR (d_6-DMSO): δ 174.1, 171.4, 168.2, 157.4, 130.1, 128.6, 114.3, 66.5, 57.0, 54.1, 51.9, 35.6, 30.1, 29.9, 24.3, 18.3, 17.1. ISMS 381 (MH^+), 282.

8-Isopropyl-6,9-dioxo-2-oxa-7,10-diaza-bicyclo[11.2.2]heptadeca-1(16),13(17),14-triene-11-carboxylic Acid Methyl Ester (15). The zwitterion (**14**) (30 mg, 0.079 mmol) and BOP (45 mg, 0.10 mmol, 1.2 equiv) were dissolved in DMF (8 mL) and stirred at room temperature for 5 min. DIPEA (100 μL, 0.56 mmol) was added, and stirring was continued overnight. The solvent was evaporated, and the residue was dissolved in EtOAc and washed with 2 M HCl, $NaHCO_3$, brine, dried over $MgSO_4$, and evaporated. The residue was purified by rp-HPLC (38% MeCN, 62% H_2O, 0.1% TFA, R_t 6.0 min) giving a white powder (17 mg, 59%) after lyophilization. ^{1}H NMR (300 MHz, $CDCl_3$): δ 7.14−7.07 (m, 1H), 6.95−6.81 (m, 3H), 5.79 (d, J = 10.2 Hz, 1H), 5.54 (d, J = 8.5 Hz, 1H), 5.10 (m, 1H), 4.51 (m, 1H), 4.28 (m, 1H), 3.82 (s, 3H), 3.66 (t, J = 8.2 Hz, 2H), 3.46 (dd, J = 13.7, 6.4 Hz, 1H), 2.58 (dd, J = 13.7, 11.3 Hz, 1H), 2.32−2.26 (m, 2H), 2.13−1.84 (m, 2H), 1.73 (m, 1H), 0.82 (apparent t, J = 6.5 Hz, 6H). ^{13}C NMR ($CDCl_3$): δ 172.1, 170.9, 170.7, 159.0, 131.9, 130.0, 128.0, 118.2, 115.7, 67.7, 58.8, 52.6, 51.7, 38.0, 31.9, 30.7, 24.8, 18.8, 18.4.

8-Isopropyl-6,9-dioxo-2-oxa-7,10-diaza-bicyclo[11.2.2]heptadeca-1(16),13(17),14-triene-11-carboxylic Acid (1). The methyl ester (**15**) (17 mg, 0.047 mmol) was dissolved in MeOH (3 mL), and then $LiOH\cdot H_2O$ (10 mg in water (1 mL)) was added. The solution was stirred at room temperature for 1 h, and was then acidified with TFA (1 drop). The solvent was evaporated, and the residue was purified by rp-HPLC (27% MeCN, 73% H_2O, 0.1% TFA, R_t 6.5 min) giving a white powder (15 mg, 92%) after lyophilization. ^{1}H NMR (300 MHz, d_6-DMSO): δ 7.87 (d, J = 9.9 Hz, 1H, Tyr-NH), 6.75 (d, J = 9.1 Hz, 1H, Val-NH), 7.03−6.94 (m, 2H), 6.73−6.67 (m, 2H), 4.74 (m, 1H, Tyr αCH), 4.29 (m, 1H), 4.15 (m, 2H), 3.63 (dd, J = 9.1, 8.1 Hz, 1H, Val αCH), 3.20 (dd, J = 13.2, 5.6 Hz, 1H), 2.54 (dd, J = 13.2, 12.6 Hz, 1H), 2.29 (m, 1H), 1.95−1.74 (m, 2H), 1.65 (m, 1H), 1.54 (m, 1H), 0.73 (d, J = 6.7 Hz, 3H), 0.68 (d, J = 6.7 Hz, 3H). ISMS 349 (MH^+). ^{1}H NMR (500 MHz, 90% H_2O/10%D_2O): δ 7.98 (d, J = 10.0 Hz, 1H), 7.18−7.12 (m, 2H), 7.03 (dd, J = 8.5, 2.1 Hz, 1H), 6.89 (dd, J = 8.5, 2.7 Hz, 1H), 6.81 (dd, J = 8.5, 2.7 Hz, 1H), 4.39 (m, 1H), 4.26 (m, 1H), 3.57 (apparent t, J = 9.1 Hz, 1H), 3.41 (dd, J = 13.7, 6.1 Hz, 1H), 2.65 (dd, J = 13.2, 12.0 Hz, 1H), 2.45 (m, 1H), 2.19 (m, 1H), 1.99−1.92 (m, 2H), 1.66 (m, 1H), 0.77 (d, J = 6.7 Hz, 3H), 0.71 (d, J = 6.7 Hz, 3H).

General Method for the Deprotection of Macrocyclic Acids (2−6) by Hydrogenation. 9*S*-Isopropyl-7,10-dioxo-2-oxa-8,11-diaza-bicyclo[12.2.2]octadeca-1(17),14(18),15-triene-12*S*-carboxylic Acid (2). A solution of the benzyl ester (**9**, n = 5) (3.0 g, 6.6 mmol) in MeOH (75 mL) was hydrogenated over 10% Pd−C, 2 atm, room temperature for 3 h. The catalyst was filtered off, and the solvent was removed in vacuo giving the carboxylic acid as a white powder (2.4 g, 100%). ^{1}H NMR (300 MHz, d_6-DMSO): δ 8.08 (d, J = 9.8 Hz, 1H), 7.34 (d, J = 9.3 Hz, 1H), 7.10 (dd, J = 8.5, 1.9 Hz, 1H), 7.02 (dd, J = 8.5, 1.9 Hz, 1H), 6.76 (dd, J = 8.5, 2.4 Hz, 1H), 6.66 (dd, J = 8.5, 2.4 Hz, 1H), 4.62 (m, 1H), 4.14−3.67 (m, 2H), 3.97 (m, 1H), 3.16 (dd, J = 13.2, 4.0 Hz, 1H), 2.53 (apparent t J = 12.8 Hz, 1H), 2.14 (m, 1H), 1.82 (m, 1H), 1.63 (m, 1H), 1.61−1.07 (m, 4H), 0.79 (d, J = 6.7 Hz, 3H), 0.73 (d, J = 6.7 Hz, 3H). ^{1}H NMR (300 MHz, CD_3OD): δ 8.35 (d, J = 9.9 Hz, 1H tyr NH), 7.47 (d, J = 9.3 Hz, 1H, Val-NH), 7.19 (dd, J = 8.5, 2.2 Hz, 1H, ArH), 7.00 (dd, J = 8.2, 2.2 Hz, 1H, ArH), 6.85 (dd, J = 8.4, 2.6 Hz, 1H, ArH), 6.76 (dd, J = 8.2, 2.6 Hz, 1H, ArH), 4.87−4.76 (m, 1H, tyr αH), 4.29−4.19 (m, 1H, CH_2OAr), 4.14−4.02 (m, 1H, CH_2OAr), 4.00 (d, J = 8.4 Hz, 1H, val αH (NH exchanged)), 3.35 (dd, J = 13.5, 4.3 Hz, 1H, tyr βH), 2.62 (dd; J = 13.5, 12.7 Hz, 1H, tyr βH), 2.20−2.07 (m, 2H, CH_2CO), 1.88−1.80 (m, 2H, val βH and CH_2), 1.60−1.25 (m, 3H, CH_2), 0.90 (d, J = 6.8 Hz, 3H, CH_3), 0.84 (d, J = 6.7 Hz, 3H, CH_3). ^{13}C NMR (d_6-DMSO): δ 172.9, 171.1, 170.1, 154.9, 131.3, 130.1, 129.1, 118.3, 117.2, 67.9, 56.9, 52.2, 36.5, 34.8, 31.4, 25.6, 21.6, 18.9, 18.6. ^{13}C NMR (CD_3OD): δ 174.93, 174.35, 172.48, 156.66, 132.56, 131.46, 130.56, 119.63, 119.40, 69.36, 59.54, 54.18, 38.50, 36.46, 32.89, 27.24, 22.84, 19.54, 19.04. HRMS m/e 362.1841 calc. for $C_{19}H_{26}N_2O_5$ 362.1842.

10*S*-Isopropyl-8,11-dioxo-2-oxa-9,12-diaza-bicyclo[13.2.2]nonadeca-1(18),15(19),16-triene-13*S*-carboxylic Acid (3). ^{1}H NMR (300 MHz, d_6-DMSO): δ 8.12 (d, J = 9.5 Hz, 1H, Tyr-NH), 7.25 (d, J = 9.1 Hz, 1H, Val NH), AA′XX′ system, 7.06 (m, 2H, $J_{AX} + J_{AX'}$ = 8.5 Hz, ortho to CH_2), 6.73 (m, 2H, $J_{AX} + J_{AX'}$ = 8.5 Hz, ortho to O), 4.62 (m, 1H, Tyr-αCH), 4.24−4.01 (m, 2H, OCH_2), 3.97 (dd, J = 9.1, 7.8 Hz, Val-αCH), 3.13 (dd, J = 13.5, 4.2 Hz, Tyr-βCH), 2.57 (dd, J = 13.5, 12.7 Hz, Tyr-βCH), 2.19−2.06 (m, 1H, H-7′), 1.95−1.84 (m, 1H, H-7′), 1.78 (m, 1H, Val-βCH), 1.65−0.90 (e, 6H, H-4′, H-5′ and H-6′), 0.80 (d, J = 6.7 Hz, Val-γCH_3), 0.72 (d, J = 6.7 Hz, 3H, Val-γCH_3). ^{13}C NMR (CD_3OD): δ 174.6, 174.5, 172.7, 158.8, 131.3, 130.7, 117.6, 68.7, 59.1, 54.1, 38.1, 35.9, 33.2, 31.1, 26.3, 26.1, 19.6, 18.8. ISMS: m/z 377 (MH^+). HRMS m/e 376.1998 calc. for $C_{20}H_{28}N_2O_5$ 376.1998.

11-Isopropyl-9,12-dioxo-2-oxa-10,13-diaza-bicyclo[14.2.2]eicosa-1(19),16(20),17-triene-14-carboxylic Acid (4). ^{1}H NMR (500 MHz, d_6-DMSO): δ 8.07 (d, J = 9.3 Hz, 1H, Tyr-NH), 7.34 (d, J = 9.3 Hz, 1H, Val-NH), 7.08 (d, J = 8.5 Hz, 2H), 6.72 (d, J = 8.5 Hz, 2H), 4.54 (m, 1H), 4.09 (m, 1H), 4.06−3.95 (m, 2H), 3.09 (dd, J = 13.6, 3.7 Hz, 1H), 2.63 (dd, J = 13.6, 12.4 Hz, 1H), 2.04 (m, 1H), 1.84 (m, 1H), 1.75 (m, 1H), 1.60 (m, 1H), 1.52 (m, 1H), 1.43−1.23 (m, 3H), 1.20−1.04 (m, 2H), 0.93 (m, 1H), 0.81 (d, J = 6.8 Hz, 3H), 0.74 (d, J = 6.8 Hz, 3H). ISMS 391 (MH^+), 781 ($2MH^+$).

12-Isopropyl-10,13-dioxo-2-oxa-11,14-diaza-bicyclo[15.2.2]-heneicosa-1(20),17(21),18-triene-15-carboxylic Acid (5). ^{1}H NMR (300 MHz, d_6-DMSO): δ 8.24 (d, J = 8.9 Hz, 1H, Tyr-NH), 7.44 (d, J = 9.2 Hz, 1H, Val-NH), 7.11 (d, J = 8.2 Hz, 2H), 6.74 (d, J = 8.2 Hz, 2H), 4.49 (m, 1H), 4.20−3.94 (m, 3H), 3.07 (dd, J = 14.0, 3.0 Hz, 1H), 2.69 (dd, J = 14.0, 12.5 Hz, 1H), 2.11 (m, 1H), 1.91 (m, 1H), 1.77 (m, 1H), 1.60−1.42 (m, 2H), 1.42−1.31 (m, 2H), 1.31−1.10 (m, 2H), 0.98 (m, 1H), 0.84 (d, J = 6.8 Hz, 3H), 0.78 (d, J = 6.8 Hz, 3H). ISMS 405 (MH^+), 809 ($2MH^+$).

15-Isopropyl-13,16-dioxo-2-oxa-14,17-diaza-bicyclo[18.2.2]tetracosa-1(23),20(24),21-triene-18-carboxylic Acid (6). ^{1}H NMR (300 MHz, d_6-DMSO): δ 8.26 (d, J = 8.6 Hz, 1H, Tyr-NH), 7.62 (d, J = 9.1 Hz, 1H, Val-NH), 7.12 (d, J = 8.2 Hz, 2H), 6.73 (d, J = 8.2 Hz, 2H), 4.35 (m, 1H), 4.15 (m, 1H), 4.06−3.82 (m, 2H), 3.01 (broad d, J = 13.9 Hz, 1H), 2.75 (broad dd, J = 13.2, 11.4 Hz, 1H), 2.20−1.77 (m, 4H), 1.75−1.60 (m, 2H), 1.55−1.09 (m, 16H), 0.85 (d, J = 6.7 Hz, 3H), 0.80 (d, J = 6.7 Hz, 3H). ISMS: m/z 447 (MH^+).

Acknowledgment. The authors thank the Australian Research Council and the National Health and Medical Research Council of Australia for partial funding of this work.

Supporting Information Available: Plots of NMR temperature-dependent chemical shifts for **2** and **3**, graph of $^3J_{NH-CH\alpha}$ coupling constants versus ring size, spectra showing relative deuterium exchange rates of amide protons for (**3**). Table of NOE derived distance and $^3J_{NH-CH\alpha}$ derived ϕ-angle restraints used for calculating the solution structure of (**1**) (PDF). This material is available free of charge via the Internet at http://pubs.acs.org.

JA0256461